OPEN ACCESS

SciCELL

RESEARCH PAPER

COMPARISON OF FINISHING MILLING STRATEGIES USING TOPOGRAPHY OF THE MACHINED SURFACE

Ján Varga[1]*, Peter Ižol[1], Ľuboš Kaščák[1], Marek Vrabel[2], Andrzej Kubit[3]

[1] Technical University of Košice, Faculty of Mechanical Engineering, Košice, Slovakia
[2] Technical University of Košice, Faculty of Mechanical Engineering, Prototyping and Innovation Centre, Košice, Slovakia
[3] Rzeszów University of Technology, Faculty of Mechanical Engineering and Aeronautics, Rzeszów, Poland

*Corresponding author: jan.varga@tuke.sk, Tel.: 055/6023523, Department of Technology, Materials and Computer Supported Production, Faculty of Mechanical Engineering, Technical University of Košice, Mäsiarska 74, 040 01 Košice, Slovakia

ABSTRACT

The plastics processing and injection molding industry is known for the fact that the future molded part contains a variety of geometric shapes and, in some cases, free surfaces. To produce these shapes, knowledge of CAM systems is required to enable the programmer to select the necessary milling strategies designed to achieve the best possible quality and dimensional accuracy. However, it is equally necessary to understand and appreciate the effect of each strategy and which strategy is best suited for a given type of surface. The paper compares finishing milling strategies by evaluating the topography of the machined surface. The material was AlCu4Mg aluminium alloy, where Constant-Z and Spiral strategy – circle-type finishing strategies were selected for the production process. Surface topography analysis was evaluated and compared at three different heights of the produced part with respect to the tool contact with the machined surface, which showed a variation in toolpaths and therefore also in the quality of machining. The surface topography results demonstrated the Constant Z strategy to be the more suitable strategy for producing the shaped surface, which achieved uniform toolpaths over the whole height of the part.

Keywords: machining, strategies, topography, effective tool diameter, radial depth

INTRODUCTION

Achieving dimensional and geometric accuracy as well as the focus on overall surface quality is still the number one parameter in various industries such as the automotive, aerospace and plastics industries. In the field of plastics processing, the milling process is mainly used in the production of molds, dies, etc. [1]. In the process of manufacturing various parts from simple shapes to complex parts, molds and dies, where it is important to achieve the desired part quality, CAM systems have been applied as a very suitable tool that offers a wide choice of different strategies for 3-axis or multi-axis machining [2]. However, the selection of the right strategy to achieve the required geometric shape or free-form surface holds an equally important role. These are the factors that ultimately lead to the required surface quality, which may include achieving the desired surface roughness, surface topography, tolerance, dimensional accuracy, etc. [3,4].

These requirements raise questions about how to achieve them. It is necessary to know the manufacturing process itself as well as the technology, and if the parts are being manufactured on CNC machines, the suitability of milling strategies and cutting conditions [5]. Computer numerical control (CNC) is a flexible, productive and the most efficient method of manufacturing to produce complex shapes [6]. Since the choice of milling strategies is conditioned by the shape of the part to be manufactured, it is not always easy to choose them correctly. Several facts must be considered, such as the type of machine used, i.e., 3-axis or 5-axis machining, the type of milling strategy, the cutting conditions, and the precision to be achieved, among others. Last but

not least is the geometry and shape of the part to be produced. Different strategies are suitable for each curve and surface, and the direction of machining is also important, be it descending or ascending. All of the factors have an influence on the quality and the resulting surface topography.

In practice, especially in the production of molds and dies, it is necessary to produce combinations of different surfaces, convex, concave, or free surfaces. Therefore, the importance of selecting the milling strategy intended for finishing is justified and it is necessary to know which of the strategies is appropriate to use for finishing a given surface. In the case of the production of the abovementioned surfaces, not only the selection of the appropriate strategy but also the contact point of the tool with the workpiece plays an equally very important role, as it changes during the production process with respect to the machined area and thus influenced, in particular, the roughness and topography of the surface [7]. The most commonly used milling strategies include zig-zag, offset, spiral, radial, constant Z and others. The selection of the strategy along with the generation of toolpaths allows the final shape of the part to be achieved [8-10]. When machining shapes such as convex, concave, or free-form surfaces, ball-end cutting tools are most commonly used, which by their geometry, allow this required shape to be achieved.

In the manufacturing process, the surface topography is the result of the tool geometry used, the cutting conditions and, most importantly, a factor known as the overlap of the toolpaths, which affects the scallop height and, therefore, the surface roughness of the machined part [11-12]. When evaluating the surface topography, not only the toolpaths can be observed on the surface of the machined part, but also the negative influences

that may affect the surface quality can be observed as well. In the case of convex, concave, or freeform shapes, these are mostly areas where zero cutting speed is achieved in the manufacturing process. These are mostly areas where the tool has a perpendicular position with respect to the machined part [13,14]. Due to the effect of this tool position on the machined surface, the degraded quality can be manifested by the appearance of various plastic deformations, a process called ploughing, grooves, etc. [15].

The effects of strategies such as linear, offset and spiral were compared in the work of Sadeghi et al. [16], who focused on the analysis of the microhardness of steel specimens with a convex shape. Ozturk et al. [17] compared the effect of 5 different machining strategies on a sample containing convex and concave curves. The objective of their research was to compare the machined surface with the surface obtained in simulation, the surface roughness and to analyze the surface texture with respect to the given strategy. It was conducted without further attention to the point of contact of the tool with the machined surface. The result was that the Constant Z strategy obtained the best roughness values.

Similarly, Scandiffio et al. [18] analyzed the contact relationship between tool and workpiece with respect to the machining direction, where they obtained a worse surface quality for the descending milling of steel samples. However, none of the authors dealt with surface topography to document the tool-workpiece contact point in the machining process. Wojciechowski et al. [19] analyzed the method of vibration estimation in freeform milling, where the result was that the length of tool alignment has a significant influence on this parameter.

The evaluation of milling strategies for convex surfaces was also carried out by Shaghayegh et al. where the radial strategy achieved the best surface texture and the helical strategy the worst one [20]. The research conducted by Tuysuz et al. [21] demonstrated the most suitable value of effective cutting speed and this was in the region where the tool cuts approximately tangential to the machined surface. When machining in the downward direction, material deformation in the form of a notch effect occurred. The low cutting speed results in maximum vibration in the machining process, which is undesirable from the point of view of surface quality. Therefore, also in this case, the correct choice of milling strategy plays an important role, in which we have to consider the contact of the tool with the machined surface [22-23]. The influence of milling strategies on the topography and surface roughness was analyzed by Kowalczyk [24], who compared four strategies in the machining of aluminum material. The result was that the best roughness values were obtained with a circular tool path. Hao et al. [25] state that the surface topography is influenced not only by the plastic deformation of the machined surface, but also by the vibrations generated during the manufacturing process.

The relationship of tool to workpiece contact in freeform machining was investigated by Arruda et al. [26], who evaluated three contact points in machining, descending, ascending, and machining through the center of the tool. In his work, Toth [27] compared the results obtained from the simulation in a CAM system with the toolpaths on machined samples. Mali et al. [28] described some gaps requiring further research in the area of freeform milling, such as tool inclination, three-dimensional surface roughness, surface topography, or residual stresses.

In three-axis milling, the tool axis (Z-axis) is fixed relative to the workpiece surface, so only the feed direction can be examined and changed by the user's CAM. The effective tool diameter and the actual cutting speed depend on the inclination of the surfaces (in 3-axis machining). This dependence affects the quality of the machined surface. Also, to meet the requirements for machining accuracy, the axis movement must be coordinated. The definition of synchronous motion of multiple axes states that each axis must traverse the distance of each segment by a position command at the same time. It is a great challenge to maintain synchronous motion in complex machining of freeform surfaces [29-31]. In the case of the assumption that a curved surface consists of different small curvature segments with different normal vectors, machining such a surface is complicated. The trajectory is divided into sub-segments to achieve the accuracy requirement, where these segment positions are transferred as a command in the form of program code to the NC machine.

The machining process includes a parameter known as cycle time, which includes the time it takes for the machine to read one line of NC code and then transfer that data to the machine motion. The second aspect is the time in which the control unit needs to correct the machine motion such as position, speed or acceleration [32]. Different toolpaths are generated in the machining process using linear interpolation, which is defined as the path between two following cutting tool positions (CL). In a CAM system, it is possible to define a tolerance zone also known as chord error, which modifies the segments of the toolpath. If the user sets the tolerance zone smaller, the toolpath becomes more similar to the CAD model [33]. When a CNC machine creates a toolpath consisting of multiple small segments (for example, when milling freeform shapes), the CNC has to calculate many NC blocks in a short time. If the CNC is unable to perform that volume of calculations to achieve the program feed rate, the CNC will reduce the feed rate to make process capabilities suitable. This is the reason why the machining time calculated by the CAM system becomes incorrect and the actual machining time is longer [34].

Several papers have addressed the application of different milling strategies in manufacturing, but only a small number have taken a closer look at the effect of milling strategy on convex, concave, or free surfaces, focusing on the tool-workpiece contact and its topography [35]. The choice of aluminium alloy was based on its wide use in the industrial field. Al-Cu-Mg alloys have many excellent attributes. Industry manufacturers are seeking novel ways and resources to achieve desired qualities for the structural components [36-38]. Therefore, the aim of this paper was to evaluate and compare two specific strategies on the quality of the machined surface by comparing and evaluating different surface topographies at different heights of the manufactured part. The justification for the evaluation of surface topography at different heights of the fabricated part lies in the tool contact with the workpiece, which is different with respect to the effective tool diameter.

The aim of the research was to contribute to scientific knowledge by investigating tool contacts at three different heights, using two milling strategies and under downward milling conditions.

MATERIAL AND METHODS

Experimental procedure

For the experimental procedure, two samples of the machined surface were produced. The sample design was created in the CAD system Solidworks and tool path generation for the machining process was defined in the system SolidCAM.

For the production, a 3-axis milling machine EMCO mill 155 was used, where the maximum spindle rotation is 5000 RPM. The material for the production was aluminum alloy (AlCu4Mg) with mechanical and chemical properties as shown in **Table 1** and **Table 2**.

Table 1 Mechanical properties of the AlCu4Mg material

Tensile strength [MPa]	Yield strength [MPa]	Hardness [HB]
101.89	86.69	90.20

Table 2 Mechanical properties of the AlCu4Mg material

Cu	Mg	Fe	Si	Mn	Ti	Zn	Al
4.30	0.79	0.26	0.24	0.3	0.04	0.04	balance

Roughing, semi-finish and finish operations are mostly used for shaping milled surfaces in the machining process. The machining operations used in the experimental research are shown in **Fig. 1.**
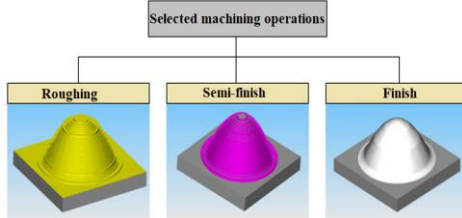
Fig. 1 Selected machining operations

Roughing and semi-finish operations were the same for all three samples to achieve the same surface texture. Of all operations, the finishing operation is the most difficult, because, in the milling process, the contact tool-material cutting speed and chip formation are changed.

The cutting parameters with the tool description used for the production are shown in **Table 3**. A carbide ball end-mill was used for the finishing operation, where a BT-40 rigid system with a mechanical collet chuck was used with a 40 mm tool overhang. Parameters for the individual operations were chosen based on the tool manufacturer's recommendations. For the cooling mineral oil-based emulsion coolant was used in the production. The test samples' dimensions were 65 x 65 x 40 mm.

Table 3 Selected cutting parameters with tool description

Tool diameter	Cutting speed [m.min^{-1}]	Feed per tooth [mm]	Spindle frequency [RPM]	Tool producer	Tool code
End Mill D18	270	0.125	4800	Korloy	AMS2018S
End Mill D8	123	0.029	4900	ZPS-FN	273618.080
Ball End Mill D6	92.4	0.022	4900	ZPS-FN	511418.060

For the milling process of the shaped surfaces, the following input data were defined.
• Roughing operation – end mill tool D18 mm, two interchangeable cutter plates marked APXT11T3PDR-MA, depth of cut a_p = 3 mm, radial depth a_e = 3 mm, toolpath tolerance T = 0.1 mm, surface allowance P = 0.5 mm
• Semi-finishing operation – end mill D 8 mm with two-flute cutters marked as 273618.080, cutting material HSS Co8, depth of cut ap = 0.5 mm, radial depth ae = 0.5 mm, strategy Constant Z, toolpath tolerance T = 0.1 mm, surface allowance P = 0.2 mm
• Finishing operation – ball end mill D 6 mm with two-flute cutters marked 511418.060, cutting material HSS Co8, radial depth a_e = 0.25 mm, toolpath tolerance T = 0.01 mm, scallop height SH = 0.01 mm

For the experimental procedure, the following methods were evaluated:
1. Machined surface analyses in CAM system SolidCAM. Simulations of machined surfaces created in Solid Verify were compared to actual samples produced.
2. Surface topography comparison and evaluation using digital microscope Keyence VHX-5000.

Each CAM system includes some possibilities to verify a machined surface. It also offers a lot of different strategies for 3 and 5-axis milling to machine different types of surfaces.

In our case strategy, two finish strategies were compared and evaluated. In the beginning, the machining process starts with roughing and semi-finishing operation. **Fig. 2** shows the machined surface in simulation mode Solid Verify and **Fig. 3** shows the real shape after machining.
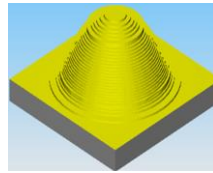
Fig. 2 Roughing operation - simulation
Fig. 3 Roughing operation – real machining
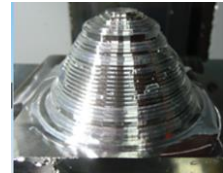
The comparison shows that the simulation shape and tool paths obtained corresponded with the real shape milling. After the roughing operation, it was possible to visually observe an irregular surface and the semi-finishing operation was used to remove it. The simulated machined surface after the semi-finish operation shown in **Fig. 4** is compared with the real machined surface in **Fig. 5**.
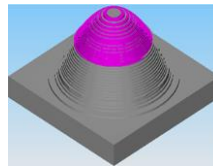
Fig. 4 Semi-finish operation – simulation
Fig. 5 Semi-finish operation – real machining
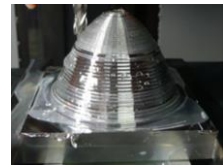
After the semi-finishing operation, similar surfaces were obtained. A surface allowance 0.2 mm was left for the finishing operation. To examine the relationship of milling strategies to surface quality, Constant Z strategy and Spiral-circle strategy were used.

The simulation of the finishing operation using Constant Z strategy as pictured in **Fig. 6** can be compared with the real machining as shown in **Fig. 7**. The finishing operation of the Spiral-circle strategy in the simulation mode is shown in **Fig. 8** and the real machining using the Spiral-circle strategy is shown in **Fig. 9**.
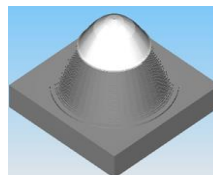
Fig. 6 Finish operation: Constant Z strategy – simulation
Fig. 7 Finish operation: Constant Z strategy – real machining
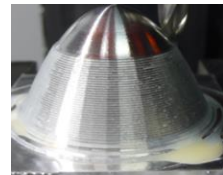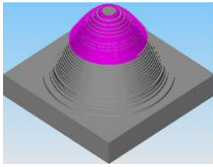
Fig. 8 Finish operation: Spiral-circle strategy – simulation

Fig. 9 Finish operation: Spiral-circle strategy – real machining

Individual comparisons show that tool paths generated using CAM system corresponded with the real machined surfaces.

Topography observation

Surface topography is the result of many factors, including vibration during the cutting process, which have the most significant effect on surface topography. These were the distances from the highest point of the sample surface downwards of 7.5 mm, 15 mm and 22.5 mm. At each of these heights, there was a change in the effective diameter of the tool relative to the machined surface, where the value depends on the axial depth of cut and the curvature of the workpiece surface.

A digital microscope was used to observe the surface elements at the specified heights as shown in **Fig. 10 to Fig. 15**. The coloured areas in all the figures represent contour lines, giving a better overview of the height location of the tool marks. The photographic part of the figures (right) shows a realistic view of the given surface element.

Grooves are visible on all sample surface elements, separating the individual cuts. It is assumed that the cause of the grooves is the method of grinding the cutting edge of the finishing tool. The cutting edge was not ground by a rolling motion of the grinding tool along the cutting edge, but the grinding tool was displaced in height by a step change in the setting angle. This resulted in the approximation of a hemispherical shape by a series of low conical surfaces.

The individual elements of the surfaces at three different heights using the Constant Z strategy are shown in **Fig. 10 to Fig. 12**.
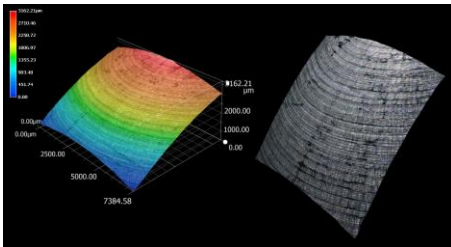
Fig. 10 Examined element surface at a height of 7.5 mm, Constant Z strategy
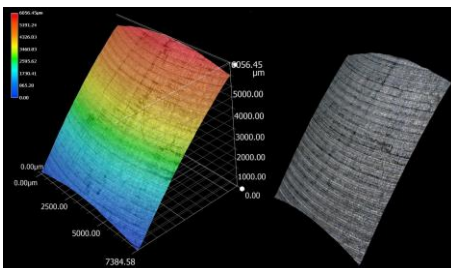
Fig. 11 Examined element surface at a height of 15 mm, Constant Z strategy
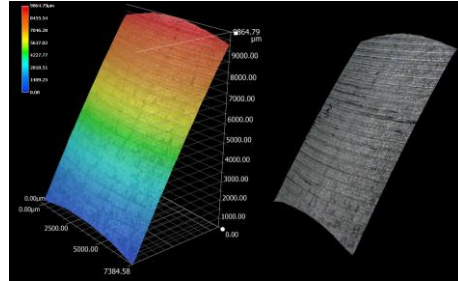
Fig. 12 Examined element surface at a height of 22. Mm, Constant Z strategy

The individual elements of the surfaces at three different heights using the Spiral- circle strategy are shown in **Fig. 13 to Fig. 15.**
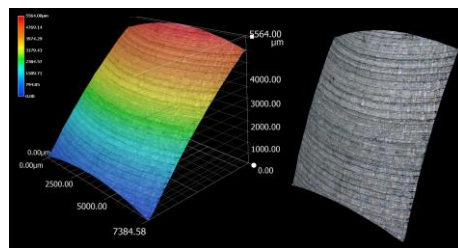
Fig. 13 Examined element surface at a height of 7.5 mm, Spiral-circle strategy
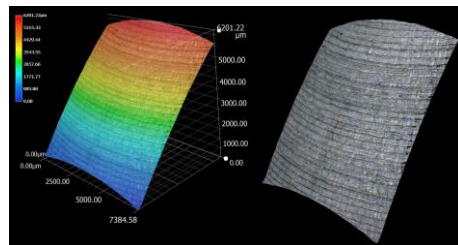
Fig. 14 Examined element surface at a height of 15 mm, Spiral-circle strategy
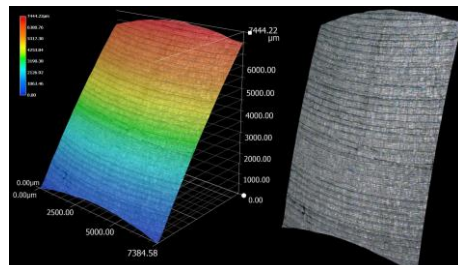
Fig. 15 Examined element surface at a height of 22 mm, Spiral-circle strategy

Examples of the detail at 50x magnification on one of the surface topography elements with respect to the 22.5 mm height at which the machined surface was observed for the Constant Z strategy are documented in **Fig. 16** and for the spiral circle strategy in **Fig. 17**. The tool grooves (toolmarks), arranged along

the contours, are clearly visible. The tool grooves (toolmarks), arranged along the contours, are clearly visible. The lighter areas represent individual chip removals (dimples), indicating a change in surface texture. It can be assumed that the cutting edge of the ball milling cutter vibrated irregularly during the spiral circle milling strategy. The toolpath will thus no longer correspond to the ideal machined surface, which may result in poor surface quality, and roughness and cause undercutting of the machined surface.
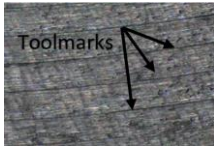
Fig. 16 Surface texture detail for strategy Constant Z
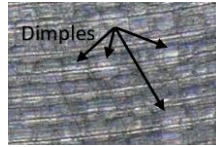
Fig. 17 Surface texture detail for Spiral-circle

From the details, it is possible to see the difference in toolpaths due to the influence of tool contact in the relationship between the tool and the machined surface. Better surface topography can be observed with the Constant Z strategy, which is visible and different from the Spiral-circle strategy.

The individual details show that under ideal conditions (no cutting vibrations and tool deformations), the toolpath is in line with the ideal machined surface and produces a uniform and periodic surface topography along the feed. This results in toolmarks arranged in contours that are clearly visible.

At distances of 7.5 mm, 15 mm and 22.5 mm from the highest point of the sample surface downwards, measurements were made indicating the distances between each radial depth of cut a_e in the downward machining direction **Fig. 18** – Constant Z strategy and **Fig. 19** Spiral-circle strategy. In general, as the curvature of the surface increases, the contact area of the tool with the workpiece increases and therefore the effective diameter of the tool increases as well.
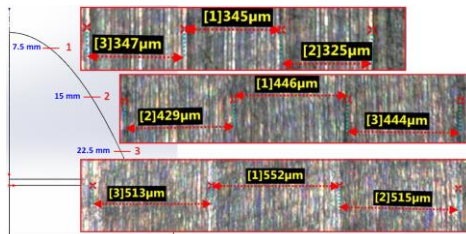
Fig. 18 Radial depth comparison for three heights, Constant Z strategy
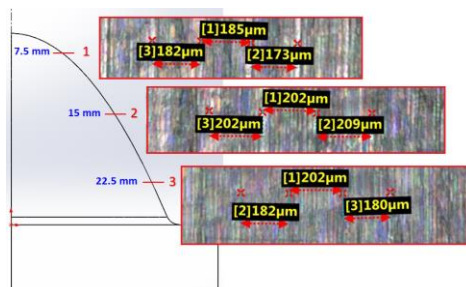
Fig. 19 Radial depth comparison for three heights, Spiral-circle strategy

In milling, the contact area between the tool and the workpiece changes due to the curvature of the workpiece as shown in **Fig. 18.** By applying the Z-constant strategy, the assumption of a larger effect of the effective tool diameter on the machined area was confirmed, where at distances from the highest point, the radial depth of cut a_e increased in the downward direction. However, for the Spiral-circle strategy, this assumption was not proved.

CONCLUSION

The surface topography of the produced part of AlCu4Mg aluminium alloy was evaluated at three different heights and compared with respect to the tool contact with the machined surface and the selected milling strategy. Descending milling direction was selected. The following conclusions were reached:

The results of the individual comparisons showed that tool paths generated using CAM system corresponded to the actual machined surfaces.

The topography of the surfaces resulted in visible grooves on the machined samples, separating the individual cuts. The cutting edge was moved in height during machining when the setting angle was changed in steps. This resulted in the approximation of a hemispherical shape by a series of low conical faces.

It was possible to see the difference in toolpaths due to the influence of tool contact in the relationship between the tool and the machined surface. A better surface topography was obtained with the Constant Z strategy.

In the Constant Z strategy, the toolpath was in line with the ideal machined surface and produced a uniform and periodic surface topography along the feed. This resulted in highly visible toolmarks arranged in contours.

At distances from the highest point, the radial depth of cut a_e increased in the downward direction due to the influence of the Constant Z strategy. For the Spiral circle strategy, this assumption was not proved, which could be caused by the influence of the tool vibration on the machined surface.

REFERENCES

1. J. Varga, T. Tóth, P. Frankovský, Ľ. Dulebová, E. Spišák, I. Zajačko, J. Živčák: Applied Science, 11(5), 2021, 2353. https://doi.org/10.3390/app11052353.
2. M. Boujelbene, A. Moisan, N. Tounsi, B. Brenier: International Journal of Machine Tools and Manufacture, 44(1), 2004, 101-107. https://doi.org/10.1016/j.ijmachtools.2003.08.005.
3. A. Razavykia, S. Iranmanesh, A. Esmaeilzadeh: International Journal of Mechanical, Aerospace, Industrial, Mechatronic and Manufacturing Engineering, 11(9), 2017, 1475–1479.
4. L. Rongrong, F. Yang, W. Xiaodong: Machines, 10(5), 2022, 331. https://doi.org/10.3390/machines10050331.
5. K. Nadolny, W. Kapłonek: Measurement Science Review, 14(4), 2014, 204-212. https://doi.org/10.2478/msr-2014-0028.
6. Z. Grešová, P. Ižol, M. Vrabeľ, Ľ. Kaščák, J. Brindza, M. Demko: Applied Science, 12(9), 2022, 4421 https://doi.org/10.3390/app12094421.
7. J. Varga, E. Spišák, I. Gajdoš, P. Mulidrán: Advances in Science and Technology Research Journal, 16(6), 2022, 267–274. https://doi.org/10.12913/22998624/156817.

8. R. Ali, M. Mia, A. Khan, W. Chen, M. Gupta, C. Pruncu: Materials, 12(7), 2019, 1013. https://doi.org/10.3390/ma12071013.
9. J. Varga, J. Stahovec, J. Beňo, M. Vrabeľ: Advances in Science and Technology Research Journal, 8(22), 2014, 37–41. https://doi.org/10.12913/22998624.1105163.
10. D. Misra, V. Sundararajan: Geometric and Algorithmic Aspects of Computer-Aided Design and Manufacturing, 2003, 265-280. https://doi.org/10.1090/dimacs/067/10.
11. Y. Mizugaki, M. Hao, K. Kikkawa, T. Nakagawa: Manufacturing Technology, 50(1), 2001, 69-72.
https://doi.org/10.1016/S0007-8506(07)62073-3.
12. H.Y. Feng, H. Li: Computer-Aided Design, 34(9), 2002, 647-654. https://doi.org/10.1016/S0010-4485(01)00136-1.
13. C. Liu, C.Z. Ren, G.F. Wang, Y.W. Yang, L. Zhang: Journal of Mechanical Science and Technology, 29(4), 2015, 1723-1730. https://doi.org/10.1007/s12206-015-0345-1.
14. S. Chiang, C. Tsai, A. Lee: Journal of Materials Processing Technology, 47, 1995, 231-249. https://doi.org/10.1016/0924-0136(95)85001-5.
15. J. Varga, T. Tóth, Ľ. Kaščák, E. Spišák: Applied Science, 12(20), 2022, 10638. https://doi.org/10.3390/app122010638.
16. M.H. Sadeghi, H. Hassanpour, S. Shajari, A. Rasti: Modares Mechanical Engineering, 15(2), 2015, 34-40.
17. E. Ozturk, L.T. Tunc, E. Budak: International Journal of Machine Tools & Manufacture, 49, 2009, 1053-1062.
https://doi.org/10.1016/j.ijmachtools.2009.07.013.
18. I. Scandiffio, A.E. Diniz, A.F. Souza: The International Journal of Advanced Manufacturing Technology, 82, 2015, 1-13.
https://doi.org/10.1007/s00170-015-7525-0.
19. S. Wojciechowski, G.M. Wiackiewicz, G.M. Krolczyk: Measurement, 129, 2018, 686-694.
https://doi.org/10.1016/j.measurement.2018.07.058.
20. S. Shaghayegh, M.H. Sadeghi, H. Hassanpour: The Scientific World Journal, 2014, 2014, 1-14.
https://doi.org/10.1155/2014/374526.
21. O. Tuysuz, Y. Altintas, H.Y. Feng: International Journal of Machine Tools & Manufacture, 66, 2013, 66-81.
https://doi.org/10.1016/J.IJMACHTOOLS.2012.12.002.
22. E. Kose, A. Kurt, U. Şeker: Journal of Materials Processing Technology, 231, 2008, 165-173.
https://doi.org/10.1016/j.jmatprotec.2007.05.019.
23. Y. Cai, L. Zhangiang, Z. Shi, Q. Song: Proceedings of the Institution of Mechanical Engineers Part B Journal of Engineering Manufacture, 231, 2015, 1-11.
https://doi.org/10.1177/0954405415608601.
24. A. Matras, R. Kowalczyk: Proceedings of SPIE - The International Society for Optical Engineering, 9290, 2014, 1-7.
https://doi.org/10.1117/12.2075081.
25. X. Hao, C. Yue, X. Liu, L. Wang: Metals, 10, 2020, 1-21.
https://doi.org/10.3390/met10091218.
26. E.M. Arruda, L.C. Brandão, S.L. Filho, J.A. Oliveira: Measurement, 47, 2014, 54-63. https://doi.org/10.1016/j.measurement.2013.08.052.
27. C.K. Toh: Journal of Materials Processing Technology, 2004; 152(3), 2004, 346–356. https://doi.org/10.1016/j.jmatprotec.2004.04.382.
28. R.A. Mali, T.V.K. Gupta: Journal of Manufacturing Processes, 62, 2021, 132-167. https://doi.org/10.1016/j.jmapro.2020.12.014.
29. H. Chuxiong, Z. Wang, Y. Zhu, M. Zhang: International Journal of Machine Tools and Manufacture, 128, 2018, 33-40.
https://doi.org/10.1016/j.ijmachtools.2018.01.001.
30. Y.Y. Ren, M. Wan, W.H. Zhang, Y. Yang: Mechanical Systems and Signal Processing, 194, 2023, 1-44.
https://doi.org/10.1016/j.ymssp.2023.110280
31. M. Kaur, D. Rattan: Computer Science Review, 47, 2023, 1-34. https://doi.org/10.1016/j.cosrev.2022.100528

32. Pessoles, X.; Landon, Y.; Rubio, W.: The International Journal of Advanced Manufacturing Technology, 47, 2010, 5-8. https://doi.org/10.48550/arXiv.1004.2354.
33. Yau, H.T.; Kuo, M.J.: Computer-aided Design, 35, 2003, 395–401. https://doi.org/10.1016/S0010-4485(02)00060-X.
34. Coelho, R.T.; Souza, A.F.; Roger, A.R.: International Journal of Advanced Manufacturing Technology, 46, 2010, 1103-1111.
http://dx.doi.org/10.1007/s00170-009-2183-8.
35. M. Vaško, M. Sága, J. Majko, A. Vaško, M. Handrik: Materials, 13(24), 2020, 5654. https://doi.org/10.3390/ma13245654.
36. A. Kubit, M. Drabczyk, T. Trzepiecinski, W. Bochnowski, Ľ. Kaščák, J. Slota: Metals, 10(5), 2020, 1-18. https://doi.org/10.3390/met10050633
37. J. Bidulská, T. Kvačkaj, R. Bidulský, M.A. Grande: High Temperature Materials and Processes, 27(3), 2008, 203-207. https://doi.org/10.1515/HTMP.2008.27.3.203
38. J. Bidulská, T. Kvačkaj, R. Bidulsky, M.A. Grande: Kovové materiály, 46(6), 2008, 339-344.